PHYSICAL REVIEW B VOLUME 11, NUMBER 2 15 JANUARY 1975

Self-consistent calculation of energy bands in aluminum*

R. A. Tawil† and S. P. Singhal
Department of Physics and Astronomy, Louisiana State University, Baton Rouge, Louisiana 70803
(Received 4 June 1974)

Results of a self-consistent linear-combination-of-atomic-orbitals calculation of the band structure of aluminum are reported. The basis set consisted of nine individual Gaussian-type orbitals (GTO's) of s symmetry, six GTO's for the radial part of each function of p symmetry, and five for the radial part of the d symmetry. This basis set is not atomic in nature. The initial Coulomb potential was constructed from the superposition of overlapping neutral-atom charge densities, the atom being in the $3s^1 3p^2$ configuration. The exchange potential was included according to a variation on the $X\alpha$ approximation. The charge density was sampled at 89 points (1/48th of the Brillouin zone). The final self-consistent potential was then utilized to compute energy levels at 505 regularly spaced points in the irreducible zone. The results are compared with other reported band structures for the same metal. The density of states was calculated and the predicted Fermi surface was analyzed in detail. No value for the exchange parameter (α) lying between 1 and 2/3 was found to reproduce the proper connectivity of the surface unless the Fermi level is shifted artificially by a small amount.

I. INTRODUCTION

The band structure and the Fermi surface of aluminum have been the subject of a large number of experimental and theoretical investigations. Of the numerous "first-principles" investigations no complete self-consistent calculation of the electronic structure of aluminum exists until the present time, and the predictions of the non-self-consistent calculations are very sensitive to the procedure followed in the construction of the crystal potential. Calculations on polyvalent copper[1,2] demonstrate the sensitivity of the features of the Fermi surface to variations in the potential caused by using different atomic functions. Sensitivity in the predictions of first-principles investigations due to such variations will be reduced if a variationally, self-consistent crystal potential is used.

We have decided to apply a recently developed form of the linear-combination-of-atomic-orbitals (LCAO) method,[3-5] successfully applied to lithium,[6] iron,[7] nickel,[8] and chromium,[9] in the study of the electronic structure of aluminum with one major modification. In this calculation the localized basis set used to construct Bloch states, as will be discussed in a subsequent section, is not atomic in nature.

A self-consistent crystal potential is obtained by an iterative procedure in which the electron distribution is sampled at 89 points in $\frac{1}{48}$th of the Brillouin zone. The exchange potential is constructed according to the $X\alpha$ method of Slater, Wilson, and Wood,[10] adjusting the value of α to obtain the "best" Fermi surface. Comparison is made with reported experimental investigations and with other reported theoretical studies.

For the rest of this section we will present a brief review of the several experimental and theoretical studies made on this metal. Experimental studies of the de Haas–van Alphen effect,[11-14] magnetoresistance,[15,16] magnetoacoustic effect,[17] cyclotron resonance,[18-20] and the Kohn effect[21] have been utilized in order to investigate the electronic structure. These measurements are consistent with a Fermi surface that overlaps the boundaries of the first Brillouin zone on each face and, in regions removed from the zone boundaries, nearly matches the free-electron model. The connectivity of the surface near the zone boundaries has been investigated by Ashcroft[22] for a phenomenological model. For this purpose a three-parameter pseudopotential interpolation scheme was set up to calculate the band structure, and the de Haas–van Alphen data of Gunnersen[11] were used for the determination of the parameters. Ashcroft found that the symmetry point W is not occupied by third-zone electrons (state W_1 is empty) and thus the third-zone portion of the Fermi surface was made up of disconnected toroidal rings, i.e., third-zone electron pockets on each face are connected, but are separated from the one on adjacent faces. The low-frequency de Haas–van Alphen measurements of Larson and Gordon[13] on the third-zone electrons substantiate this model. Anderson and Lane[14] have made corresponding measurements on the second-zone electrons and combined their measurements with those of Ref. 13 to recalculate the bands and other physical quantities of the Ashcroft model. Good agreement was achieved with the experimental cross section areas and cyclotron masses.

The theoretical investigations of the band struc-

ture of aluminum were initiated by Matyas[23] using the tight-binding method and by Antonick[24] using a modified augmented-plane-wave (APW) method. These two calculations were subject to severe limitations imposed by inadequate computational facilities. Heine[25] performed two complete band calculations with different potentials, using the orthogonalized-plane-wave (OPW) method. In the more complete of these computations the potential was generated from the charge density of Al^{+3} ions including exchange and incorporating an estimate of the effects due to correlation among ion-core electrons. The exchange between conduction and core electrons was nonlocal (l dependent), and the Coulomb potential due to the conduction electrons was calculated using three orthogonalized plane waves. The energies were finally adjusted by means of the Bohm-Pines[26] formula to account for the correlation and exchange of conduction electrons. Harrison[27] subsequently used a pseudopotential interpolation scheme to extend the band energies calculated at symmetry points by Heine into the interior of the Brillouin zone in order to obtain the Fermi surface. In 1961, Segall[28] applied the Korringa-Kohn-Rostoker (KKR) or Green's-function method to a calculation of the energy bands in aluminum. Two potentials were used. The first was that employed by Heine, modified to the muffin-tin form, and the second was a corrected version of the Heine potential given by Behringer.[29] In both calculations the Bohm-Pines contribution was omitted. Segall's calculations demonstrated the sensitivity of the topology of the Fermi surface to small changes (about 0.01 Ry) in the Fermi level. Heine's construction of the crystal potential uses one of the most fundamental techniques. However, the calculation by Harrison[27] which is based on this potential leads to a Fermi surface extending into the fourth zone. That of Segall,[28] for two potentials generated from it by introducing the specific modifications and corrections cited above, also resulted in a Fermi surface with the wrong connectivity.

Snow[30] performed two self-consistent energy-band calculations on aluminum using the APW method. The potential for the first iteration was obtained from the Hartree-Fock-Slater (HFS) atomic calculations of Herman and Skillman.[31] The self-consistency was incomplete since it allowed only partial readjustment of the core wave functions and the potential was constrained to have the muffin-tin form. Unfortunately, this calculation has an inherent systematic error and was repeated by Greisen[32] for a few $\vec{k}$ points. The energies as reported by Snow were in error up to 0.08 Ry and the predicted Fermi surface had the wrong connectivity. The most recent investigation of the band structure of aluminum was reported by Faulkner[33] using the KKR method. The potential was generated from a superposition of Al free-atom charge densities as calculated by Synek.[34] Two calculations were performed, one using the full value of the Slater free-electron exchange parameter and the other using the Kohn-Sham value, $\frac{2}{3}$. The Slater value for the exchange parameter lead to the correct connectivity of the Fermi surface while the value of $\frac{2}{3}$ did not. This calculation is not decisive for this type of potential since it was not self-consistent. Lack of self-consistency renders the results strongly dependent on the atomic wave functions used in the construction of the crystal charge density as demonstrated by such considerations on copper.[1,2]

We decided to apply the LCAO method in a computationally adequate manner to the study of the electronic structure of aluminum. The calculation, although employing a local exchange potential, is free of some limitations imposed on previous calculations through use of muffin-tin potentials or interpolation schemes.

II. METHOD

The LCAO method employed here is a variational approach to the solution of the one-electron Schrödinger equation. Thr procedure followed in this calculation is similar to that reported elsewhere,[6] and will be described only briefly here.

The wave function $\psi_n(\vec{k}, \vec{r})$ for a state of wave vector $\vec{k}$ in band n is expressed in terms of a set of one-electron functions $\phi_i(\vec{k}, \vec{r})$ satisfying the Bloch condition, and constructed from independent Gaussian orbitals. The basis set contained nine independent Gaussian-type orbitals (GTO) of s symmetry, six for the radial part of each function of p symmetry, and five for the radial part of functions of d symmetry. The Hamiltonian matrix has dimension 52×52 with this basis.

Table I shows the values of the exponents used for the three symmetries (9, 6, and 5 values for s, p, and d, respectively).

In selecting the exponents, it was observed that the energy levels at a few randomly selected $\vec{k}$ points in the zone are not sensitive to the actual values of these exponents provided that the range spanned and their relative separations are reasonable. The most extended Gaussian orbital, for a given symmetry, was selected to have a maximum in the probability density close to or beyond the boundary of the unit cell. The selection of the exponents for the s- and p-type symmetry was made from the self-consistent-field calculations performed on atomic aluminum by Veillard.[35] No

TABLE I. Exponents for the Gaussian-type orbitals.

j	$l=0$	$l=1$	$l=2$
1	15000.	200.	25.
2	5000.	40.	9.
3	500.	9.	2.1
4	90.	1.2	0.5
5	16.	0.44	0.125
6	5.	0.135	
7	1.5		
8	0.38		
9	0.12		

such calculations involving d states for this atom have been performed. Several (six) sets of exponents for the d symmetry were tried. No variation in the overlap matrix resulted when the value of the largest exponent was varied between 15.0 and 50.0. The value of 0.125 for the smallest exponent leads to a maximum in the probability density close to the cell boundary, and the other three exponents were selected to span the range.

The calculation was begun by constructing a crystal potential from a superposition of overlapping neutral-atom charge densities, the atoms assumed to be in the $3s^1 3p^2$ configuration. The wave functions used in forming the atomic charge density were taken from the Hartree-Fock self-consistent-field calculations of Clementi,[36] which are linear combinations of Slater-type orbitals. Contributions from the first 15 shells of neighbors ensured convergence in the direct lattice summation for the Hamiltonian and overlap matrices while the reciprocal lattice summation was carried out to 24 000 unique vectors. Energy levels and wave functions were determined for this potential and used to initiate an iterative procedure leading to self-consistency. In this process corrected Fourier coefficients of the Coulomb potential are calculated using wave functions of the occupied states at 89 points in $\frac{1}{48}$th of the Brillouin zone resulting from the previous iteration. The exchange parameter α was set equal to $\frac{2}{3}$. Subsequently, the calculations were repeated for $\alpha = 0.75$ and 1.0.

A corrected exchange potential was obtained as follows: The charge in the Fourier coefficients of the charge density was averaged over directions of the reciprocal-lattice vector $\vec{K}$, and the resulting Fourier series were summed numerically to determine the change in the charge density in an atomic cell. This change was added to the starting charge density and the cube root extracted. Revised Fourier coefficients of the exchange potential were then obtained.

It was found that only the Fourier coefficients pertaining to the lowest 20 rotationally independent reciprocal-lattice vectors were appreciably affected by the self-consistency procedure coefficients for large $\vec{K}$'s describe the charge density inside an atomic core and do not vary significantly. The criteria used to define adequate degree of self-consistency was that the Fourier coefficients of the Coulomb potential should be stable to 0.0005 Ry. The coefficients of the exchange potential were observed to converge somewhat more rapidly than those for the Coulomb potential. The values of 19 Fourier coefficients are listed in Table II. After the self-consistency had been determined to the desired accuracy, energies and wave functions were computed at 505 regularly spaced points in $\frac{1}{48}$th of the Brillouin zone. The density of states were computed by the Gilat-Raubenheimer[37] method.

III. RESULTS AND DISCUSSION

The calculated band structure is shown in Fig. 1 for several symmetry directions. It is evident from the shape of the $E(\vec{k})$ curves (Δ, Λ, and Σ directions) that, away from the zone boundaries the energy bands approximate closely those of a free electron. Deviations occur for regions near the zone surface, especially in the $K \rightarrow W$ and $W \rightarrow X$ directions, where gap effects are manifest and where the degeneracies of the free-electron

TABLE II. Some Fourier coefficients of potentials. The self-consistent Coulomb and exchange coefficients for the smallest 19 reciprocal-lattice vectors are listed. The change in these quantities resulting from the iterative process is given.

$\vec{K}$	$V_c(\vec{K})$	$\Delta V_c(\vec{K})$	$V_{ex}(\vec{K})$	$\Delta V_{ex}(\vec{K})$
(1, 1, 1)	−0.45149	−0.01840	−0.13855	−0.00521
(2, 0, 0)	−0.37589	−0.02078	−0.04963	−0.00288
(2, 2, 0)	−0.23723	−0.01357	−0.01794	+0.00045
(3, 1, 1)	−0.19266	−0.00973	−0.05617	+0.00151
(2, 2, 2)	−0.18214	−0.00877	−0.06197	+0.00191
(4, 0, 0)	−0.15140	−0.00650	−0.05093	+0.00361
(3, 3, 1)	−0.13547	−0.00530	−0.02681	+0.00452
(4, 2, 0)	−0.13100	−0.00494	−0.01924	+0.00468
(4, 2, 2)	−0.11608	−0.00358	+0.00045	+0.00448
(3, 3, 3)	−0.10715	−0.00273	+0.00309	+0.00355
(5, 1, 1)	−0.10715	−0.00274	+0.00309	+0.00355
(4, 4, 0)	−0.09512	−0.00164	−0.00544	+0.00119
(5, 3, 1)	−0.08916	−0.00113	−0.01134	−0.00027
(6, 0, 0)	−0.08734	−0.00097	−0.01276	−0.00071
(4, 4, 2)	−0.08734	−0.00098	−0.01276	−0.00071
(6, 2, 0)	−0.08075	−0.00047	−0.01467	−0.00211
(5, 3, 3)	−0.07643	−0.00018	−0.01237	−0.00271
(6, 2, 2)	−0.07509	−0.00010	−0.01108	−0.00282
(4, 4, 4)	−0.07016	+0.00017	−0.00475	−0.00287

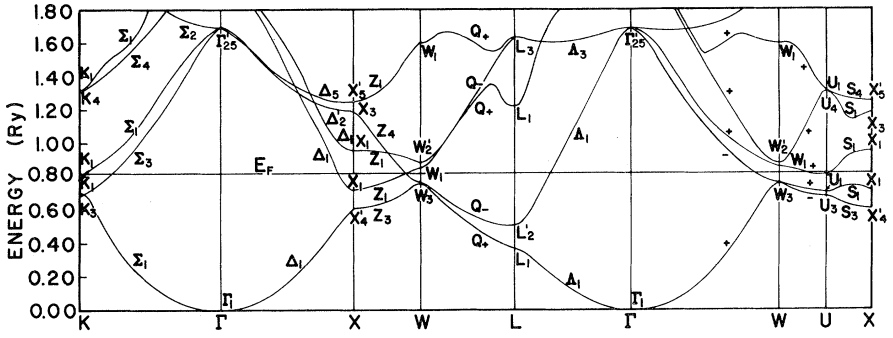

FIG. 1. Band structure of aluminum along certain symmetry directions.

model are lifted. The energy levels at high-symmetry points are reported in Table III and compared with the corresponding results obtained from other theoretical investigations. Of particular interest is the order of the levels at the points L and W. In contrast to all other investigations the L_1 level (with 1 and $xy+yz+xz$ as the basis) is lower in energy than the pure p-like level L_2'. Since the difference in energy between the L_2' energy obtained from this calculation and those of other calculations are no larger than 0.04 Ry and those for L_1 are around 0.2, one can conclude that s-d mixing for this point (L) is very important. Strong mixing effects are also found at the point W. At this point we find that the W_1 level (basis 1, $3y^2-r^2$) is the intermediate level between $W_3(xy, yz;\ x_2z)$ and $W_2'(y, z^2-x^2)$.

When our results are compared with the corresponding values reported by Anderson and Lane,[12] we observe that our band is narrower by about 0.028 Ry. When columns (viii) and (ix) are compared one can conclude that the effect of the iterative procedure is to decrease the bandwidth, to increase the splitting between the levels at the point X, decrease the splitting between the levels at L and K, and not to affect those at W significantly.

The calculated density of states is shown in Fig. 2 and is characterized by a free-electron shape for energies up to 0.2 Ry, a shoulder between 0.2 and 0.5 Ry, and the region between 0.5 and the Fermi level (0.816 Ry) is characterized by a local maximum at 0.625 Ry and a local minimum at 0.7 Ry. The shoulder may result from distortions in the first band near the zone boundary and the structure may be attributed to the band gaps near the zone boundary at the L point (L_2' and L_1 level). The local maximum at 0.625 Ry corresponds to the band gap near the zone boundary at X (X_4' and X_1 level), and the relative minimum at 0.70 Ry corresponds to the band gap around the points U or K (levels K_3 and K_1). The structure

TABLE III. Energy levels at high-symmetry points in Ry. Column i: Heine, Ref. 25, as reported by Segall; ii: Segall, Ref. 28, using Heine's potential; iii: Segall, Ref. 28, using Behringer potential; iv: Greisen, Ref. 32, $\alpha=1$; v: Greisen, Ref. 32, $\alpha=\frac{2}{3}$; vi: Faulkner, Ref. 33, $\alpha=1$; vii: Faulkner, Ref. 33, $\alpha=\frac{2}{3}$; viii: present calculation, non-self-consistent, $\alpha=\frac{2}{3}$; ix: present calculation, self-consistent, $\alpha=\frac{2}{3}$; x: Anderson and Lane, Ref. 19.

Energy levels	i	ii	iii	iv	v	vi	vii	viii	ix	x
Γ_1	0.000	0.000	0.000	0.000	0.000	0.000	0.000	0.000	0.000	0.000
X_4	0.592	0.629	0.622	0.597	0.607	0.6063	0.6138	0.6138	0.6128	0.623
X_1	0.717	0.703	0.698	0.679	0.678	0.6766	0.6849	0.7337	0.7212	0.744
L_2'		0.482	0.483	0.467	0.477	0.4770	0.4715	0.5122	0.5124	0.493
L_1		0.530	0.512	0.491	0.489	0.4872	0.5058	0.3719	0.3706	0.526
W_1	0.949	0.968	0.923	0.866	0.857	0.8270	0.9204	0.8789	0.8608	0.953
W_2'	0.826	0.812	0.819	0.808	0.818	0.8211	0.8008	0.8911	0.8839	0.881
W_3	0.774	0.786	0.776	0.750	0.760	0.7620	0.7642	0.7603	0.7619	0.793
K_3	0.699	0.710	0.699	0.673	0.684	0.6852	0.6886	0.6854	0.6858	0.708
K_1	0.742	0.757	0.723	0.705	0.714	0.7148	0.7073	0.7166	0.7117	0.756
K_1	1.075	0.842	0.802	0.766	0.762	0.7619	0.7918	0.8232	0.8130	0.837
E_F		0.833	0.833	0.8134 [a]		0.8115	0.8198	0.8371	0.8164	0.866

[a] As calculated by Faulkner, Ref. 33.

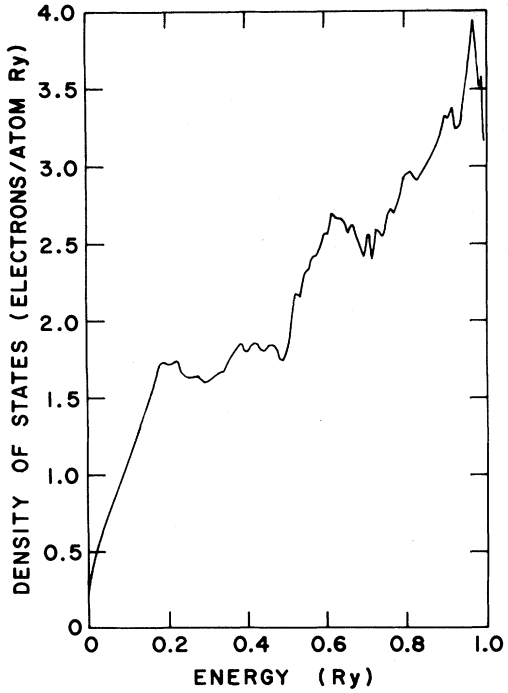

FIG. 2. Density of states.

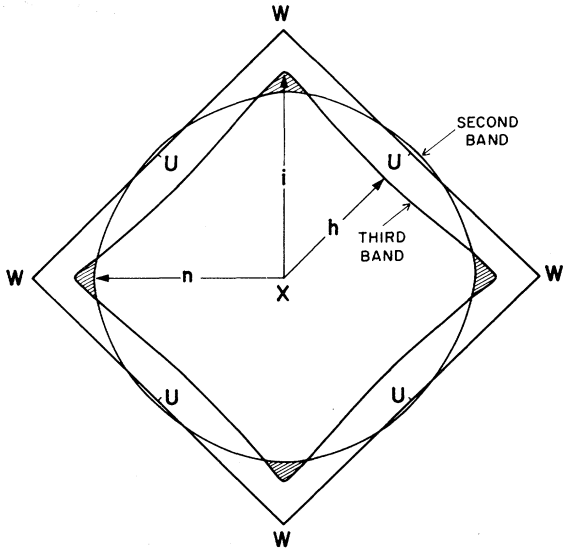

FIG. 3. Fermi surface in third zone: section in a (1, 0, 0) plane through $(W-X-U)$ for $E_F=0.816$ Ry. Shaded area corresponds to the region where second and third zones are empty. The Larson and Gordon (Ref. 13) nomenclature is adopted for the orbits.

close to the Fermi level can be attributed to the shape of the bands in the X-W and W-K directions in the vicinity of the point W. At the Fermi level the density of states obtained from this calculation is 2.95 states/(Ry atom) compared to the values 2.998, 2.72, and 2.32 obtained by Faulkner,[33] Snow,[30] and Anderson *et al.*,[14] respectively.

Our Fermi-surface calculations yield a large second-zone hole surface which has small portions in contact with the zone face. This is in disagreement with experimental results which show that this surface should be closed. The prediction of contact is quite sensitive to the calculated Fermi energy. A displacement of the Fermi energy upwards by 0.01 Ry is sufficient to remove the contact. The Fermi-surface portions in the third zone consist of disconnected electron pieces as shown in Fig. 3. We have calculated cross sections in the (100) plane through X and in the (110) and (111) planes through the points K and L, respectively; these pieces have the general features of those predicted by Ashcroft.[22]

Cross-sectional areas for the different orbits in units of $(2\pi/a)^2$ ($a=7.635$ atomic units) are reported in Table IV and can be compared with the

TABLE IV. Fermi-surface cross-section areas in units of $(2\pi/a)^2$. Orbits are labeled according to Larson and Gordon, Ref. 13.

		Areas in units of $(2\pi/a)^2$					
Orbit	Axis	Empty lattice	Three-parameter model	Expt		This calculation $E_F=0.8164$ (Ry)	This calculation $E_F=0.8350$ (Ry)
ψ_1	[110]	1.728	1.698	1.709	±0.002	1.625	1.699
ψ_1	[111]	1.898	1.623	1.609	±0.008	1.620	1.620
ψ_1	[100]	2.84 [a]	2.60	2.66	±0.08	2.781 [a]	2.645
ξ	[100]	0.3501	0.3474	0.3472	±0.0003	•••	0.3468
γ_5	[110]	0.0212	0.01114	0.0112	±0.0001	0.0031	0.0108
γ_5	[111]	0.0254	0.01355	0.135	±0.0002	0.0021	0.1360
β	[100]	•••	0.00179	0.00182	±0.00008	•••	0.0020

[a] Orbit has been closed along the zone boundary.

values reported by Anderson *et al.*[14] and the values of the free-electron model. The dimensions of the intersections of the Fermi-surface with some symmetry lines are defined and reported in Table V in units of $(2\pi/a)$.

We also confirm from this calculation that the cross-sectional areas of the third zone pieces, particularly the ξ, β, and γ_5 orbits, are extremely sensitive to small variations in the Fermi level. This has been demonstrated in the last column of Tables IV and V, where a Fermi level of 0.835 Ry brings the cross-sectional area to an excellent agreement with the experimental values for all orbits. As pointed out previously, a Fermi level of 0.835 Ry will effect the proper connectivity in the (100) plane as demonstrated in Fig. 4 for the third-zone electrons, and will eliminate the open orbit for the second-zone hole surface.

Recent work on the band structure of copper indicates that the value of the exchange parameter α which gives the best agreement between theory and experiment in regard to the Fermi surface properties is $\alpha = 0.77$, significantly larger than the value $\frac{2}{3}$ used here.[38] In order to see whether a larger value of α would lead to an improved Fermi surface by eliminating the contact between the major hole surface and the zone face we repeated the self-consistent calculations with $\alpha = 0.75$ and $\alpha = 1.0$. No improvement was noted, the region of contact being slightly larger in those cases than for $\alpha = \frac{2}{3}$.

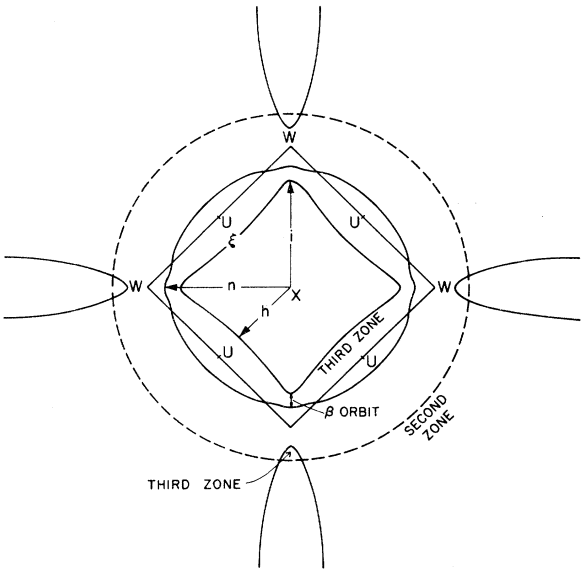

FIG. 4. Fermi surface in third zone: section in a (1, 0, 0) plane through $(W-X-U)$ for a Fermi energy of 0.835 Ry. See caption of Fig. 3.

TABLE V. Locations of the intersections of the Fermi surface with some symmetry lines in units of $2\pi/a$.

Plane	Orbit	Intersection length	Direction	$E_F = 0.816$ (Ry)	$E_F = 0.835$ (Ry)
		b	$\Gamma \rightarrow X$	0.905	0.892
	ψ_1	c	$\Gamma \rightarrow W$	0.967	0.931
		d	$\Gamma \rightarrow K$	0.831	0.803
(1, 0, 0)					
		n	$X \rightarrow W$ [a]	0.376	0.422
	ξ	h	$X \rightarrow U$	0.281	0.257
		i	$X \rightarrow W$ [b]	0.417	0.391
		e	$\Gamma \rightarrow U$	0.728	0.718
	ψ_1	f	$\Gamma \rightarrow L$	0.603	0.590
(1, 1, 0)					
		l	$K \rightarrow X$	0.073	0.096
	γ_5	l'	$K \rightarrow \Gamma$	0.008	0.051
		m	$K \rightarrow L$	0.005	0.028
	ψ_1	g	$\Gamma \rightarrow (\frac{3}{4}, \frac{3}{8}, \frac{3}{8})$	0.656	0.639
(1, 1, 1)					
		j	$L \rightarrow U$	0.609	0.585
	γ_5	p	$W \rightarrow U$	0.280	0.147

[a] Second-zone intersection.
[b] Third-zone intersection.

ACKNOWLEDGMENT

It is a great pleasure to thank Professor Joseph Callaway for suggesting the problem and for many helpful discussions throughout the course of this work.

---

*Supported in part by the U. S. Army Research Office.

†Present address: Battelle Memorial Institute, 505 King Ave., Columbus, Ohio 43201.

[1]J. S. Faulkner, H. L. Davis, and H. W. Joy, Phys. Rev. 161, 656 (1967).

[2]H. L. Davis, J. S. Faulkner, and H. W. Joy, Phys. Rev. 167, 601 (1968).

[3]E. Lafon and C. C. Lin, Phys. Rev. 152, 597 (1966).

[4]R. C. Chaney, T. K. Tung, C. C. Lin, and E. Lafon, J. Chem. Phys. 52, 361 (1970).

[5]J. Callaway and J. L. Fry, in *Computational Methods in Band Theory,* edited by P. M. Marcus, J. F. Janak, and A. R. Williams (Plenum, New York, 1971), p. 571.

[6]W. Y. Ching and J. Callaway, Phys. Rev. B (to be published).

[7]R. A. Tawil and J. Callaway, Phys. Rev. B 7, 4242 (1973).

[8]J. Callaway and C. S. Wang, Phys. Rev. B 7, 1096 (1973).

[9]J. Rath and J. Callaway, Phys. Rev. B 8, 5398 (1973).

[10]J. C. Slater, T. M. Wilson, and J. H. Wood, Phys. Rev. 179, 28 (1969).

[11]E. Gunnersen, Philos. Trans. R. Soc. Lond. A 251, 85 (1958).

[12]M. G. Priestly, Philos. Mag. 7, 1205 (1962).

[13]C. O. Larson and W. L. Gordon, Phys. Rev. 156, 703 (1967).

[14]J. R. Anderson and S. S. Lane, Phys. Rev. B 2, 298 (1970).

[15]E. S. Borovik and V. G. Volotskaya, Zh. Eksp. Teor. Fiz. 48, 1554 (1965) [Sov. Phys.-JETP 21, 1041 (1965)].

[16]R. A. Parker and R. J. Balcomb, Phys. Lett. A 27, 197 (1968).

[17]G. N. Kamm and H. V. Bohm, Phys. Rev. 131, 111 (1963).

[18]T. W. Moore and F. Spong, Phys. Rev. 125, 846 (1962).

[19]F. Spong and A. K. Kip, Phys. Rev. 137, A431 (1965).

[20]S. W. Hui and J. A. Rayne, J. Low Temp. Phys. 12, 49 (1973).

[21]R. Stedman and G. Nilsson, Phys. Rev. Lett. 15, 634 (1965).

[22]N. W. Ashcroft, Philos. Mag. 8, 2055 (1963).

[23]Z. Matyas, Philos. Mag. 30, 429 (1948).

[24]E. Antonick, Czech. J. Phys. 2, 18 (1953).

[25]V. Heine, Proc. R. Soc. Lond. A 240, 340, 354, 361 (1957).

[26]D. Pines, Solid State Phys. 1, 368 (1955).

[27]W. A. Harrison, Phys. Rev. 118, 1182 (1960).

[28]B. Segall, Phys. Rev. 124, 1797 (1961).

[29]R. E. Behringer, J. Phys. Chem. Solids 5, 145 (1958).

[30]E. C. Snow, Phys. Rev. 158, 683 (1967).

[31]F. Herman and S. Skillman, *Atomic Structure Calculations* (Prentice-Hall, Englewood Cliffs, N.J., 1963).

[32]F. C. Greisen, Phys. Status Solidi 25, 753 (1968).

[33]J. S. Faulkner, Phys. Rev. 178, 914 (1969).

[34]M. Synek, Phys. Rev. 131, 1572 (1963).

[35]A. Veillard, Theor. Chim. Acta. 12, 405 (1968).

[36]E. Clementi, IBM J. Res. Dev. 9, 2 (1965).

[37]G. Gilat and L. J. Raubenheimer, Phys. Rev. 144, 340 (1966).

[38]J. F. Janak, A. R. Williams, and V. L. Moruzzi, Phys. Rev. B 6, 4367 (1972).